

## A computer simulation investigation into the stability of the $AB_2$ superlattice in a binary hard sphere system

By M. D. ELDRIDGE, P. A. MADDEN

Physical Chemistry Laboratory, Oxford University, South Parks Road,  
Oxford OX1 3QZ, UK

and D. FRENKEL

FOM-Institute for Atomic and Molecular Physics, Kruislaan 407, NL-1098 SJ  
Amsterdam, The Netherlands

(Received 24 November 1992; accepted 23 December 1992)

The thermodynamic stability of the binary hard-sphere  $AB_2$  superlattice structure has been confirmed by means of computer simulations. This is consistent with the results of experimental studies of suspensions of hard-sphere colloidal particles. A fit of the Helmholtz free energy surface for the region in phase space where  $AB_2$  is found to be stable is presented, together with results for the  $c/a$  ratio of this hexagonal crystal.

### 1. Introduction

In the recent experiments of Bartlett *et al.* [1, 2] unusual superlattice structures were observed forming from binary mixtures of colloidal particles. These include  $AB_2$ , similar to the crystallographic aluminium boride ( $AlB_2$ ) structure, and  $AB_{13}$ , isomorphous to the metallic alloy  $NaZn_{13}$  with its complicated icosahedral arrangement of  $B$  atoms. The colloidal suspensions consisted of sterically stabilized polymethylmethacrylate (PMMA) spheres in a decalin/carbon disulphide medium. It has been shown that PMMA colloidal particles interact through a steep, repulsive potential closely approximating that of hard spheres [3-5]. This makes the very rich phase behaviour exhibited by these systems all the more extraordinary.

The first experiments were with spheres at a size ratio,  $\alpha = \sigma_B/\sigma_A = 0.62$  [1]. Crystalline  $AB_2$  was not observed and  $AB_{13}$  (mixed with crystals of pure  $B$ ) formed very slowly and subsequently disappeared after many months. The apparent metastability of  $AB_{13}$  at this size ratio prompted our previous computer simulation study of the thermodynamic stability of the hard-sphere  $AB_{13}$ -phase [6]. The results of the simulations showed hard-sphere  $AB_{13}$  to be stable, at least with respect to the simpler phases one would expect a binary system to adopt [7], for a range of diameter ratios,  $\alpha = 0.48-0.62$ . The calculated upper boundary to  $AB_{13}$  stability at  $\alpha = 0.62$  (for which the  $AB_{13}$  free energy is extremely similar to those of the competing phases) is consistent with the experimental metastability observed for  $AB_{13}$ . Later experiments for a size ratio,  $\alpha = 0.58$ , saw the formation of a stable  $AB_{13}$  crystal phase at a faster rate and also the emergence of small crystallites of  $AB_2$  [2]. The  $AB_{13}$  and  $AB_2$  structures have also been observed in gem opals, consisting of colloidal silica spheres [8], in binary suspensions of charge-stabilized latex spheres [9, 10] and in high-pressure inert gas mixtures as van der Waals compounds [11].

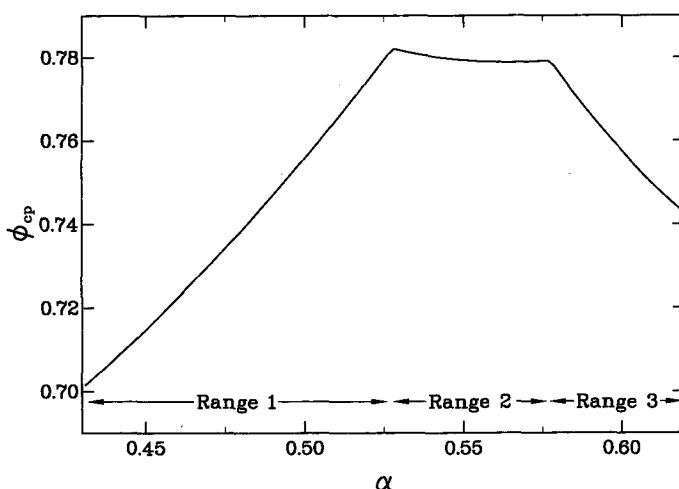


Figure 1. The space-filling curves, i.e. of maximum packing fraction, as a function of  $\alpha$  for  $AB_2$ .

A density-functional hard-sphere study has recently provided further verification of the stability of  $AB_{13}$  and  $AB_2$  in mixtures with compositions corresponding to the stoichiometry of these two phases [12]. Such calculations are free of system-size effects which may limit the reliability of simulation studies of phase equilibria. The Helmholtz free energies calculated for  $AB_{13}$  were in good agreement with our simulation values [6].

It is surprising that a 'real-life' binary hard-sphere system can arrange itself, at high density, into these complex structures. The transition is thought to be entropically driven with an increase in the free volume available to each of the spheres upon crystallization. In particular, if a crystal structure has a high close-packed density, then for lower densities its constituent particles will have a large free volume in which to move and thus a high translational entropy. On this basis, we would expect binary  $A_mB_n$  structures with close-packed densities greater than the close-packing fraction for monodisperse spheres,  $\phi_{cp}^{(1)} = 0.7405$ , to be preferred, especially at high pressures, to phase separation into coexisting monodisperse face-centred-cubic (f.c.c.) crystals of  $A$  and  $B$ . Murray and Sanders have explored the stability of several binary structures by use of this *space-filling principle* [8]. The  $AB_2$  structure is found to have close-packed packing fractions greater than  $\phi_{cp}^{(1)}$  for size ratios in the range,  $\alpha = 0.482\text{--}0.625$  (see figure 1).

Here, we report the results of an investigation into the stability of the  $AB_2$ -phase making use of the Frenkel-Ladd method for calculation of crystal-phase free energies [13] (the technique applied to a binary crystal is discussed in detail in [6]). The  $AB_2$  structure consists of alternate hexagonal layers of large and small spheres. The large spheres ( $A$ ) form close-packed layers which align directly above each other along the  $c$ -axis. The small spheres ( $B$ ) occupy the trigonal prismatic sites between these layers and form planar hexagonal rings resembling the carbon layers in graphite. In our simulations we employ a rhombic prismatic box consisting of  $6 \times 6 \times 6$  unit cells (each of which is a rhombic prism containing one  $A$  and two  $B$  particles): the total number of particles used was  $N = 648$ . The stability of a binary crystal,

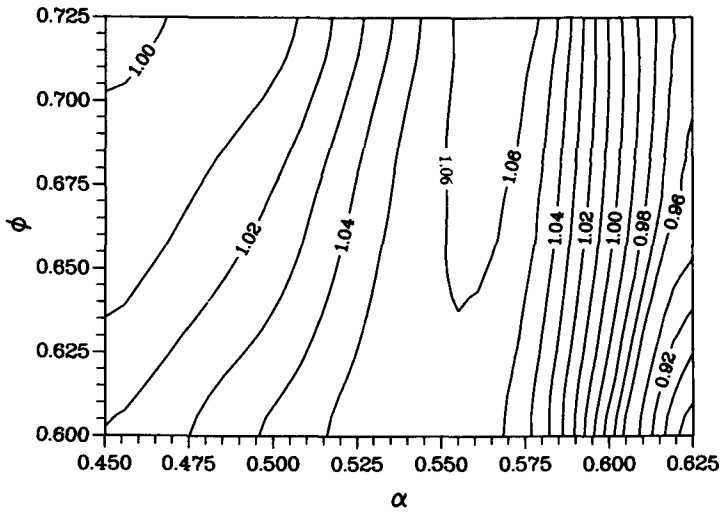


Figure 2. The  $c/a$  ratio as a function of  $\phi$  and  $\alpha$  for the strain-free  $AB_2$  crystal phase.

$A_m B_n$ , typically depends on two variables, namely the packing fraction,  $\phi$ , and the diameter ratio,  $\alpha$ . It is evident that the  $AB_2$  crystal is complicated by an additional parameter, the layer-spacing or  $c/a$  ratio. To calculate the free energy of the  $AB_2$ -phase as a function of these variables,  $\phi$ ,  $\alpha$  and  $c/a$ , would certainly be an exhausting task. However, since the experimentally observed  $AB_2$  crystals form from a binary fluid suspension, it seems likely that they are free of strain. There is only one value of  $c/a$  for each point in  $\phi, \alpha$ -phase space for which  $AB_2$  can be strain-free, so with this assumption the problem is reduced to one of two dimensions once again.

## 2. The $c/a$ ratio and free energy calculations

We have calculated the  $c/a$  ratio for strain-free  $AB_2$  as a function of  $\phi$  and  $\alpha$  within collision dynamics (MD) simulations using a simple scaling algorithm. We start the MD simulation with a reasonable guess for  $c/a$  then let the simulation proceed for a few thousand collisions monitoring the pressure components in the  $x$ -,  $y$ - and  $z$ -directions (the  $AB_2$  crystal is set up such that its principal  $c$ -axis is aligned with the box  $z$ -axis; in this scenario the pressure components  $P_{xx}$ ,  $P_{yy}$  and  $P_{zz}$  are equal to the diagonal stress tensor elements and the off-diagonal elements are zero on average). The  $xy$ -plane pressures, i.e. those acting within the  $AB_2$  crystal planes are equal ( $P_{xx} = P_{yy}$ ) and for a strain-free crystal are also equal to  $P_{zz}$ , the pressure normal to the planes. At various intervals throughout the simulation we scale the coordinates of the spheres and alter the shape of the enclosing simulation box in a manner which leads to making these pressures equal ( $P_{xx} = P_{zz}$ ). For example, if  $P_{zz} > P_{xx}$  it is obvious we need to increase the  $c/a$  ratio, i.e. elongate the rhombic box in the  $z$ -direction, while if  $P_{zz} < P_{xx}$  we must decrease  $c/a$ . This scaling is accompanied by a rescaling of particle diameters to maintain a constant packing fraction,  $\phi$ . Hence particle overlaps become a constraint on the degree of scaling one can perform in any one step. After a number of scaling steps the pressures  $P_{xx}$ ,  $P_{yy}$  and  $P_{zz}$  become almost identical and  $c/a$  is well-established. The  $c/a$  ratio calculated in this way for strain-free  $AB_2$  is plotted as a function of  $\phi$  and  $\alpha$  in figure 2.

The Frenkel–Ladd free energy calculations [13] have been supplemented by thermodynamic integration procedures to determine relative free energies within a crystal phase. Integrations have been made with respect to the packing fraction,  $\phi$  (see [6]), and size ratio,  $\alpha$  [14], to enable a more efficient ‘mapping-out’ of phase space, although the latter method does not appear to have the desired accuracy for the purposes of this study. The free energy of the binary fluid has been obtained by thermodynamic integration from the dilute gas phase. We make use of the well-known semi-empirical expression of Mansoori *et al.* [15] for the binary fluid equation-of-state.

We have fitted the  $AB_2$  excess free energies in the ranges  $\alpha = 0.425\text{--}0.625$ ,  $\phi = 0.60\text{--}0.725$ , to a function of the form

$$F^{\text{ex}} = \left( p_1 \ln y_1 + \sum_{i=2}^m p_i y_1^{i-2} \right) \left( 1 + \sum_{j=1}^n q_j \alpha^j \right) + \left( r_1 \ln y_3 + \sum_{k=2}^m r_k y_3^{k-2} \right) \times \left( 1 + \sum_{l=1}^n s_l \alpha^l \right) \tag{1}$$

where

$$y_1 = \left( \frac{\phi_{\text{cp},1}(\alpha)}{\phi} - 1 \right), \tag{2a}$$

$$y_3 = \left( \frac{\phi_{\text{cp},3}(\alpha)}{\phi} - 1 \right). \tag{2b}$$

The space-filling curves used here,  $\phi_{\text{cp},1}$  and  $\phi_{\text{cp},3}$ , for ranges 1 and 3 shown in figure 1 have been extended beyond their applicable ranges. They are given by the following equations:

$$\text{Range 1: } \alpha < 0.527, \quad \phi_{\text{cp},1} = \frac{\pi}{3\sqrt{3}}(2\alpha^3 + 1), \tag{3a}$$

$$\text{Range 3: } 0.577 < \alpha < 0.667, \quad \phi_{\text{cp},3} = \frac{\pi(2\alpha^3 + 1)}{9\sqrt{3}\alpha^2(1 + 2\alpha - 3\alpha^2)^{1/2}}. \tag{3b}$$

The function with  $m = 4$  and  $n = 2$ , i.e.

$$F_{\text{fit}}^{\text{ex}} = c_1 + c_2\alpha + c_3\alpha^2 + c_4 \ln y_1 + c_5 y_1 + c_6 y_1^2 + c_7 \alpha \ln y_1 + c_8 \alpha y_1 + c_9 \alpha y_1^2 + c_{10} \alpha^2 \ln y_1 + c_{11} \alpha^2 y_1 + c_{12} \alpha^2 y_1^2 + c_{13} \ln y_3 + c_{14} y_3 + c_{15} \alpha y_3^2 + c_{16} \alpha \ln y_3 + c_{17} \alpha y_3 + c_{18} \alpha y_3^2 + c_{19} \alpha^2 \ln y_3 + c_{20} \alpha^2 y_3 + c_{21} \alpha^2 y_3^2, \tag{4}$$

gives a reasonable fit (for a 269-point dataset the sum of square differences is 0.227) for a manageable number of coefficients. The 21 coefficients,  $c_i$ , are given in table 1.

### 3. The stability of $AB_2$

In addressing the question of the stability of the  $AB_2$ -phase we must first define the most probable competing phases for a particular point in phase space. At low densities this will certainly be the binary fluid, whereas at higher densities we would

Table 1. Coefficients for the polynomial fit of the  $AB_2$  free energy surface.

	Coefficient	Basis function
$c_1$	107.52928	1
$c_2$	-78.16360	$\alpha$
$c_3$	-214.63342	$\alpha^2$
$c_4$	-36.13625	$\ln y_1$
$c_5$	-64.43814	$y_1$
$c_6$	-25.48693	$y_1^2$
$c_7$	-164.73168	$\alpha \ln y_1$
$c_8$	137.54093	$\alpha y_1$
$c_9$	-30.01445	$\alpha y_1^2$
$c_{10}$	-191.27993	$\alpha^2 \ln y_1$
$c_{11}$	177.26623	$\alpha^2 y_1$
$c_{12}$	-34.70501	$\alpha^2 y_1^2$
$c_{13}$	1.78932	$\ln y_3$
$c_{14}$	-80.95480	$y_3$
$c_{15}$	-28.91789	$y_3^2$
$c_{16}$	7.98936	$\alpha \ln y_3$
$c_{17}$	-13.83148	$\alpha y_3$
$c_{18}$	183.23233	$\alpha y_3^2$
$c_{19}$	-24.56534	$\alpha^2 \ln y_3$
$c_{20}$	112.27400	$\alpha^2 y_3$
$c_{21}$	-93.01429	$\alpha^2 y_3^2$

expect the phase-separation of two coexisting f.c.c. crystals ( $A$  and  $B$ ). Bartlett has prescribed a simple approach to this problem [7], using approximations to the equation-of-state of the fluid (the Mansoori equation) and pure solid phases (the parametrization of Alder *et al.* [16]). These equations-of-state, when integrated with respect to volume,  $V$ , and then differentiated with respect to the number of particles of one of the species,  $N_i$ , yield the chemical potential of species  $i$ ,  $\mu_i$ , within that phase. Coexisting phases ( $\alpha$ ,  $\beta$ ) in equilibrium obey the following relations:

$$P_\alpha = P_\beta, \quad (5a)$$

$$\mu_\alpha^A = \mu_\beta^A, \quad (5b)$$

$$\mu_\alpha^B = \mu_\beta^B. \quad (5c)$$

In Bartlett's picture, the fluid mixture at high density freezes into crystalline solid phases of pure  $A$  and pure  $B$  — impurities in the solid phases are not catered for. Following this approach for a given size ratio,  $\alpha$ , we can compute a constant-volume phase diagram. An example for  $\alpha = 0.58$  is given in figure 3. Also indicated in this figure is the line of constant composition,  $X = \frac{1}{3}$ , corresponding to the  $AB_2$  stoichiometry. If we prepare a system with this overall composition, we should therefore compare the free energy of  $AB_2$  with the free energies of the following phases in order of increasing density: binary fluid ( $f$ ), fluid coexisting with solid  $A$  ( $s_A + f$ ), the eutectic state where solid  $A$  and  $B$  coexist with the fluid ( $s_A + s_B + f$ ) and the state in which the system has separated into pure solid  $A$  and pure solid  $B$  ( $s_A + s_B$ ). The free energies of those phases are shown in figure 4 for  $\alpha = 0.58$ . From this figure we can determine that  $AB_2$  is stable (for  $\alpha = 0.58$ ) for packing fractions greater than  $\phi = 0.6164$ . It should be pointed out that other phases or combinations of phases

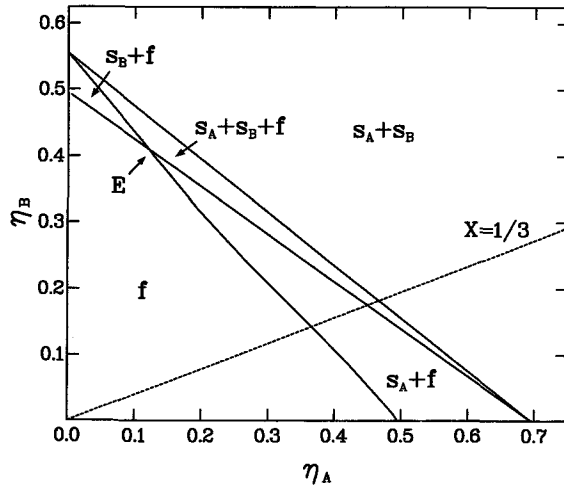


Figure 3. Constant-volume phase diagram for binary mixtures of hard spheres of diameter ratio,  $\alpha = 0.58$ , arising from the description of Bartlett [7].  $\eta_{A(B)}$  is the partial packing fraction of the large (small) spheres. The labels  $s_A$ ,  $s_B$  and  $f$  refer to the solid phase of large spheres ( $A$ ), the solid phase of small spheres ( $B$ ) and the fluid phase, respectively,  $E$  denotes the eutectic fluid. Also shown is the line of composition,  $X + \frac{1}{3}$ , corresponding to  $AB_2$ .

might be more stable here than  $AB_2$ , including a number of possible phases coexisting with the  $AB_{13}$  crystal phase. This issue will be discussed elsewhere where a more complete phase diagram with  $AB_2$  and  $AB_{13}$  regions will be presented [17]. However, in the present work the analysis is restricted to a comparison of the  $AB_2$  stability with respect to the phases listed above.

We have repeated comparisons of this nature over a wide range of diameter ratios. In figure 5 we present a 'phase diagram' showing the phase region (shaded) of thermodynamic stability of  $AB_2$  over the competing phases arising from the model

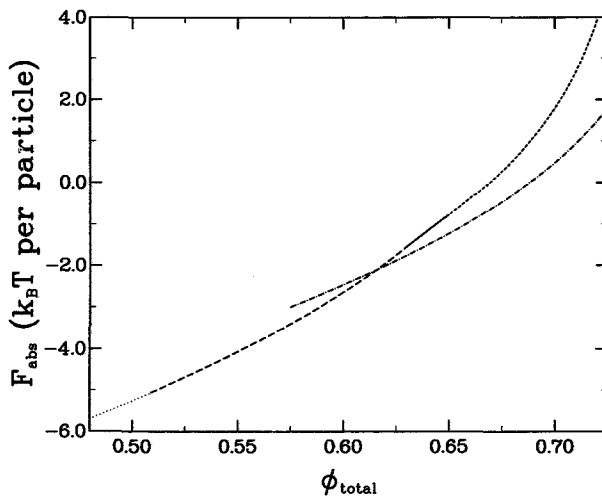


Figure 4. Absolute free energies of  $AB_2$  (- · - ·) and the phases arising from the Bartlett approach [7] for a diameter ratio,  $\alpha = 0.58$ . These phases are fluid (· · · · ·), solid  $A +$  fluid (— — —), solid  $A +$  solid  $B +$  fluid (———) and solid  $A +$  solid  $B$  (-----).

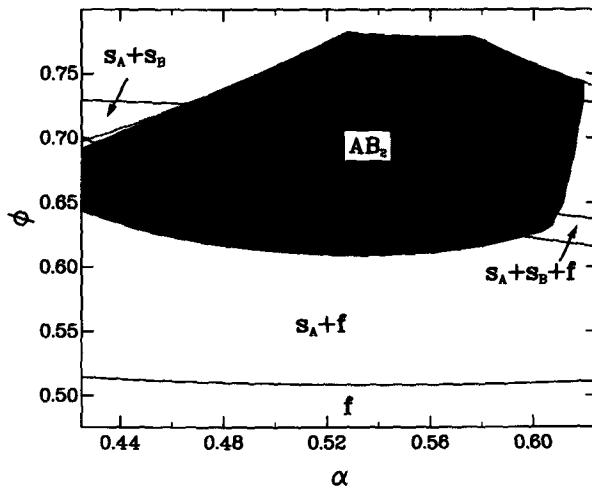


Figure 5. Phase diagram showing the region (shaded) of stability of  $AB_2$  over the phases arising from the description of Bartlett [7]. The space-filling curve for  $AB_2$  is shown as the dashed curve.

of Bartlett [7]. A measure of the stability of the  $AB_2$  phase is given by the difference in absolute free energy of  $AB_2$  and the underlying Bartlett phase (see figure 6),

$$\Delta F = F_{\text{Bartlett}}^{\text{abs}} - F_{AB_2}^{\text{abs}} \quad (6)$$

The noteworthy feature of figure 6 is that it shows that over a large domain  $AB_2$  is only just stable ( $\Delta F < k_B T/2$ , say). This suggests that the predicted stability of  $AB_2$  in the true hard-sphere system could be easily affected by other factors in real colloidal suspensions such as polydispersity or the finite range (i.e. the not quite true hard-sphere nature) of the interparticle interaction.

The phase behaviour as seen in these diagrams is consistent with the observation

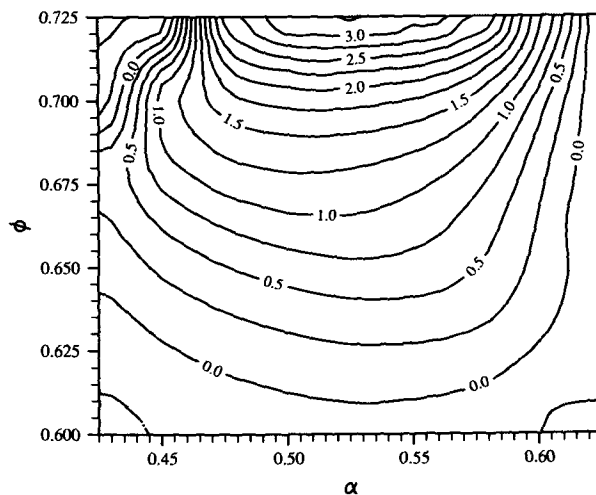


Figure 6.  $\Delta F$ , the difference between the free energy of the  $AB_2$ -phase and the competing Bartlett phases, as a function of  $\phi$  and  $\alpha$ .

of  $AB_2$  crystals in the colloidal suspensions for a size ratio,  $\alpha = 0.58$ , with a packing fraction of about  $\phi = 0.64$ . This density, and also the  $c/a$  ratio [18], were calculated from the line positions of the powder diffraction pattern. The calculated  $c/a$  ratio of 1.045 compares quite well with that computed in the equal stress-component MD simulation, a value of 1.049. Rather interestingly, the experimental suspensions prepared with an overall composition,  $X = \frac{1}{3}$  (the  $AB_2$  stoichiometry), remained amorphous, not crystallizing over several months ( $AB_2$  did crystallize, though, for the compositions,  $X = \frac{1}{3}$  and  $X = \frac{1}{7}$ ). It is clear from our phase diagram that  $AB_2$  would have been thermodynamically preferred for packing fractions in excess of  $\phi = 0.616$ . However, the samples were prepared with lower overall volume fractions than this.

We find that the upper limit to  $AB_2$  stability occurs for a size ratio,  $\alpha \simeq 0.62$ , above which it becomes less stable with respect to phase separation of pure  $A$  and  $B$  crystals. This is consistent with the absence of any observation of  $AB_2$  at  $\alpha = 0.62$  in the colloidal suspensions of Bartlett *et al.* [1, 2]. This is also in agreement with the study of Murray and Sanders [8], based on packing considerations. They showed that the  $AB_2$  structure exhibits close-packed packing fractions greater than that of a monodisperse f.c.c. phase for size ratios in the range,  $\alpha = 0.482-0.625$  (the space-filling curve for  $AB_2$  is shown in figure 1). They expect the system to form a state in which crystals of  $A$  and  $B$  have phase separated for  $\alpha < 0.482$  at high density. Our results show  $AB_2$  to be thermodynamically stable for diameter ratios as low as  $\alpha = 0.425$ . The  $s_A + s_B$  phase is reentrant though, for very high packing fractions at diameter ratios,  $\alpha < 0.468$ , with  $AB_2$  stable at lower  $\phi$ .  $AB_2$  is seen (in figure 6) to be most stable, i.e.  $\Delta F$  greatest, for diameter ratios in the range,  $\alpha = 0.48-0.575$ , at high densities. Here, the particles have a larger free volume as a result of the  $AB_2$  structure than they would have had if phase-separated into f.c.c. crystals, and so a higher entropy.

We should note that the reliability of the Mansoori equation-of-state for the fluid becomes questionable for the lower diameter ratios used. The lower packing fraction boundary on the  $AB_2$  phase diagram is particularly affected. This is because the estimated coexistence density of the binary fluid in the  $s_A + f/s_A + s_B + f$  phases is very high, and the Mansoori equation leads to an overestimate of the fluid free energy. Hence we would expect these phases to be slightly more favourable with respect to  $AB_2$  than depicted. The effect is not thought to be large since a plot of their free energies as a function of  $\phi$  shows curves which run smoothly into each other with no great differences (or 'jumps') on going from stable  $s_A + f$  to  $s_A + s_B + f$  to the  $s_A + s_B$  phase. Such 'jumps' were only evident for  $\alpha = 0.425$ .

The computations were performed on the Intel iPSC/860 parallel computer at the Daresbury Laboratory and on IBM RISC/6000 machines whose purchase was enabled by a Computer Science Initiative grant from the Science and Engineering Research Council (SERC). We thank Paul Bartlett and Peter Pusey for continuing helpful discussions and communicating useful experimental details. M.D.E. wishes to acknowledge financial support from SERC and the Royal Signals and Radar Establishment, Malvern.

### References

- [1] BARTLETT, P., OTTEWILL, R. H., and PUSEY, P. N., 1990, *J. chem. Phys.*, **93**, 1299.



- [2] BARTLETT, P., OTTEWILL, R. H., and PUSEY, P. N., 1992, *Phys. Rev. Lett.*, **68**, 3801.
- [3] PUSEY, P. N., and VAN MEGAN, W., 1986, *Nature*, **320**, 340.
- [4] LIVSEY, I., and OTTEWILL, R. H., 1989, *Colloid Polym. Sci.*, **267**, 421.
- [5] PAULIN, S. E., and ACKERSON, B. J., 1990, *Phys. Rev. Lett.*, **64**, 2663.
- [6] ELDRIDGE, M. D., MADEN, P. A., and FRENKEL, D., 1993, *Mol. Phys.*, **79**, 105.
- [7] BARTLETT, P., 1990, *J. Phys.: Condens. Matter*, **2**, 4979.
- [8] MURRAY, M. J., and SANDERS, J. V., 1980, *Phil. Mag. A*, **42**, 721.
- [9] YOSHIMURA, S., and HACHISU, S., 1983, *Prog. Colloid Polymer Sci.*, **68**, 59; *J. Physique*, **46**, Colloque C3, 115 (1985).
- [10] HACHISU, S., and YOSHIMURA, S., 1987, *Physics of Complex and Supermolecular Fluids*, edited by S. A. Safran and N. A. Clark (Wiley).
- [11] BARRAT, J. L., and VOS, W. L., 1992, *J. Chem. Phys.*, **97**, 5707.
- [12] XU, H., and BAUS, M., 1992, *J. Phys.: Condens. Matter*, **4**, L663.
- [13] FRENKEL, D., and LADD, A. J. C., 1984, *J. chem. Phys.*, **81**, 3188.
- [14] KRANENDONK, W. G. T., and FRENKEL, D., 1991, *Molec. Phys.*, **72**, 699.
- [15] MANSOORI, G. A., CARNAHAN, N. F., STARLING, K. E., and LELAND, T. W., 1971, *J. chem. Phys.*, **54**, 1523.
- [16] ALDER, B. J., HOOVER, W. G., and YOUNG, D. A., 1968, *J. chem. Phys.*, **49**, 3688; YOUNG, D. A., and ALDER, B. J., 1979, *J. chem. Phys.*, **70**, 473.
- [17] ELDRIDGE, M. D., MADDEN, P. A., and FRENKEL, D., 1993, *Nature* (submitted).
- [18] BARTLET, P., private communication.